Synthesis and Biological Evaluation of 4-Arylcoumarin Analogues of Combretastatins

Christian Bailly,*,† Christine Bal,† Pascale Barbier,‡ Sébastien Combes,§ Jean-Pierre Finet,*,§ Marie-Paule Hildebrand,† Vincent Peyrot,‡ and Nicole Wattez†

INSERM U-524 et Laboratoire de Pharmacologie antitumorale du Centre Oscar Lambret, Institut de Recherches sur le Cancer, Place de Verdun, 59045 Lille, France, UMR 6032 CNRS − Université d'Aix-Marseille 2, "Interaction entre Systèmes Protéiques et Différenciation dans la Cellule Tumorale", Faculté de Pharmacie de Marseille, 27 boulevard Jean Moulin, 13385 Marseille Cedex 5, France, and UMR 6517 CNRS − Universités d'Aix-Marseille 1 et 3, "Chimie, Biologie et Radicaux Libres" Faculté des Sciences St Jérôme, case 541, 13397 Marseille Cedex 20, France

Received May 22, 2003

A series of A-ring polymethoxylated neoflavonoids was prepared by ligand coupling reactions involving either Suzuki or Stille reactions. Cytotoxicity studies indicated a potent activity against a CEM leukemia cell line for the compounds presenting a substitution pattern related to that of combretastatin A-4. The two compounds having a 3′-OH and a 4′-OCH_3 substituents on the 4-phenyl B-ring have no effect on human topoisomerases I and II but potently inhibit, in vitro, microtubule assembly. At the cell level, the active compounds were characterized as proapoptotic agents, but they can also trigger cell death via a nonapoptotic pathway.

Among the various antimitotic agents inhibiting tubulin polymerization by interaction with the colchicine site,[1] combretastatin derivatives constitute one of the most extensively investigated group since the discovery of combretastatin A-4 (Scheme 1).[2] A number of derivatives or analogues have been prepared to improve the solubility, stability, or therapeutic index. A key structural factor for the cytotoxic activity is the presence of the cis double bond, forcing the two aromatic rings to be noncoplanar and within an appropriate distance.[2b,3,4]

In the past recent years, a number of neoflavonoid (4-phenylcoumarin) derivatives isolated from various plant sources have revealed cytotoxic properties.[5] Chemopreventive activity against cancer without cytotoxicity was observed for some derivatives.[6] As the two aromatic rings (A and B) of 4-phenylcoumarin derivatives adopt also a conformation in which they are not coplanar,[7] the structural similarity between combretastatin and neoflavonoid can be expected to lead to an activity on the colchicine site of tubulin polymerization in the case of conveniently substituted neoflavonoids. Moreover, such a structure will avoid inactivation resulting from cis-to-trans isomerization of the double bond of combretastatin derivatives. We therefore decided to investigate the synthesis of neoflavonoid analogues of combretastatin A-4 and to study their biological efficiency toward tubulin polymerization as well as potential topoisomerase inhibitors,[8] in view of the antitopoisomerase-II activity that has been reported for the structurally related isoflavonoid, genistein, and for podophyllotoxin derivatives.[9]

* Corresponding authors. C.B.: Tel, (+) 33 3 20 16 92 18; Fax, (+) 33 3 20 16 92 29; e-mail, bailly@lille.inserm.fr. J.-P.F.: Tel, (+) 33 4 91 28 89 27; Fax, (+) 33 4 91 28 87 58; e-mail, finet@srepir1.univ-mrs.fr.

† Institut de Recherches sur le Cancer.

‡ Université d'Aix-Marseille 2.

§ Universités d'Aix-Marseille 1 et 3.

Results and Discussion

Chemistry. Synthesis of 4-arylcoumarin derivatives by ligand coupling reaction of two aromatic units, the preformed coumarin ring and a conveniently activated phenyl derivative, constitutes an efficient access to the polymethoxylated derivatives.[10] Among the various synthetic methods (Stille coupling or Suzuki coupling), the method of Boland et al.[11] can be used for the synthesis of neoflavonoids containing a number of alkoxy or hydroxy groups,[12] by C-4 arylation of 4-activated coumarins with arylboronic acids in the presence of a palladium catalyst and copper(I) iodide as a cocatalyst. We used this method for the synthesis of the 5,6,7-trimethoxycoumarin derivatives **1**−**4** as well as for the synthesis of the 5,7-dimethoxy analogues **6**−**9**.

The 4-trifluoromethylsulfonyloxycoumarins **10** and **11** were easily prepared in 87−90% yield by treatment of the appropriate 4-hydroxycoumarins[13,14] with triflic anhydride.[11] Use of the benzyl-protected arylboronic acids **12**−**15** in the palladium−copper-catalyzed Suzuki coupling reaction led to the protected hydroxycoumarin derivatives **16**−**23** in good to high yields (69−96%, Table 1).

In the presence of the easily reduced benzopyrone, deprotection of the benzyloxy group by the reported selective palladium-catalyzed hydrogenolysis proved unreliable. However, selective removal of the benzyl group was performed successfully by treatment with hydrobromic acid, leading to the expected hydroxylated 4-arylcoumarins **1**−**4** and **6**−**9** in good yields (62−96%, Table 2). On the other hand, the trimethoxylated benzodioxane derivative **5** was prepared in 63% yield by the Stille palladium-catalyzed coupling of the coumarin derivative **10** with tributyl-3,4-methylenedioxyphenyltin.[15]

Biology. Cytotoxicity. A tetrazolium-based assay was applied to determine the drug concentration required to inhibit cell growth by 50% after incubation in

10.1021/jm030903d CCC: $25.00
Published on Web 10/31/2003

Scheme 1

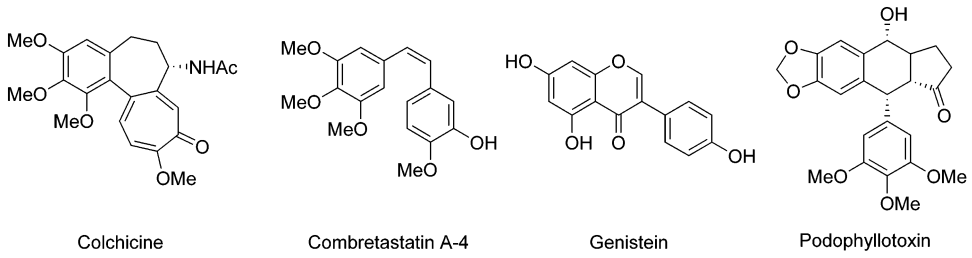

Scheme 2

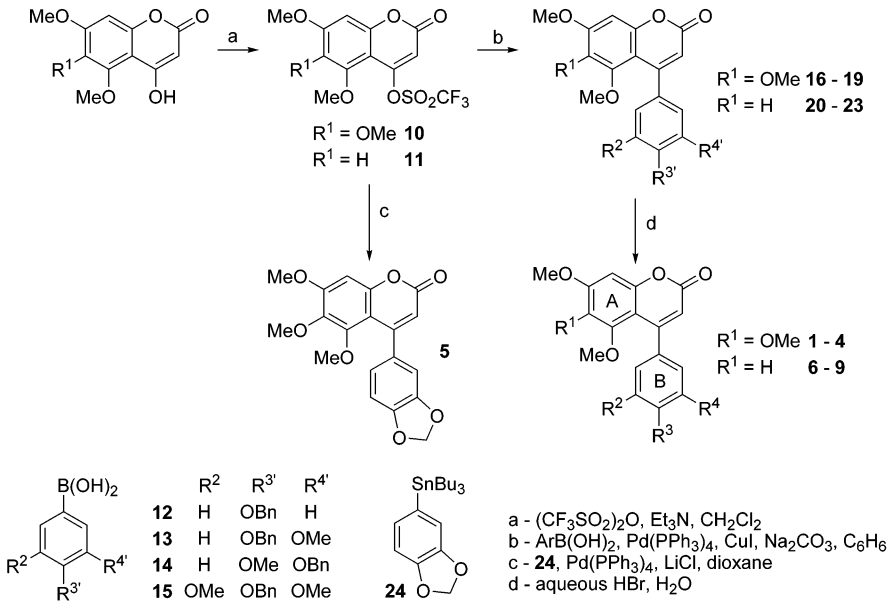

Table 1. Structures and Yields of the Products of the Suzuki Coupling Reaction

substrate	$ArB(OH)_2$	product	yield (%)	Ar
		5,6,7-OMe Substituted		
10	**12**	**16**	69	4-$BnOC_6H_4$
10	**13**	**17**	89	4-BnO-3-$MeOC_6H_3$
10	**14**	**18**	96	3-BnO-4-$MeOC_6H_3$
10	**15**	**19**	90	4-BnO-3,5-$(MeO)_2C_6H_2$
		5,7-OMe Substituted		
11	**12**	**20**	94	4-$BnOC_6H_4$
11	**13**	**21**	93	4-BnO-3-$MeOC_6H_3$
11	**14**	**22**	96	3-BnO-4-$MeOC_6H_3$
11	**15**	**23**	86	4-BnO-3,5-$(MeO)_2C_6H_2$

Table 2. Structures and Yields of the Debenzylation Reaction Products

	substituent				
product	R_1	R_2	R_3	R_4	yield (%)
6	H	H	OH	H	69
7	H	H	OH	OMe	62
8	H	H	OMe	OH	74
9	H	OMe	OH	OMe	96
1	OMe	H	OH	H	80
2	OMe	H	OH	OMe	83
3	OMe	H	OMe	OH	79
4	OMe	OMe	OH	OMe	88

the culture medium for 72 h. The calculated IC_{50} values with the CEM human leukemia cell line are collated in Table 3. Compounds **1**, **2**, **4**, **5**, and **9** were found to be inactive and a modest cytotoxic effect was observed with **6** and **7**. In sharp contrast, the two molecules **3** and **8** exhibited potent cytotoxic activities. The IC_{50} value

Table 3. Cytotoxicity

compd	**1**	**2**	**3**	**4**	**5**	**6**	**7**	**8**	**9**
IC_{50} (μM)[a]	47	54	0.52	62	>50	16	10.6	0.083	>75

[a] Drug concentration that inhibits the growth of CEM by 50% after incubation in liquid medium for 72 h. Each drug concentration was tested in triplicate, and the SE of each point is <10%.

amounts to 83 nM with **8**, which reflects a very pronounced antiproliferative activity. Parenthetically, it is worth mentioning that a similar low IC_{50} value of 81 nM was measured with compound **3** when using CEM/C2 cells selected for resistance to the topoisomerase I inhibitor camptothecin.[16] The mutation of the *top1* gene in these cells does not affect the action of the drug, and this is consistent with a nontopoisomerase dependent cytotoxicity (see below).

The position of the hydroxy and methoxy substitutents is essential for the cytotoxic effect. A priori, the A-ring dimethoxy compounds are more cytotoxic than the A-ring trimethoxy (compare **6** vs **1** and **8** vs **3**), but the most important position effect concerns the 4-phenyl B-ring. A 3′-hydroxy group is critical to maintain the cytotoxic activity. The two potent compounds **3** and **8** both bear 3′-OH and 4′-OCH_3 groups. The reverse situation 4′-OH and 3′-OCH_3, as it is the case for **2** and **7**, results in a very significant loss of activity. This is further evidenced with compounds **4** and **9**, which have also the unfavorable 4′-OH and 3′-OCH_3 and are totally inactive. The bridge conformation with the methylene dioxy compound **5** is also detrimental to the cytotoxic action. It is absolutely clear that the correct substitution

pattern for the 4-phenyl B-ring is 3′-OH and 4′-OCH_3, providing thus a precise structure−activity relationship.

The next step of our medicinal chemistry program consisted of identifying the potential target(s) for the two highly cytotoxic compounds **3** and **8**. On the basis of the structural similarity between the 4-arylcoumarin and combretastatin A-4, it was logical to investigate the effects of the compounds on tubulin polymerization. But in parallel, we also studied the effect of the different molecules against topoisomerases I and II, as different coumarin derivatives, such as genistein, have been shown to act as poisons for these DNA-manipulating enzymes.[17,18] Colchicine derivatives can also function as topoisomerase II inhibitors.[19]

Effects on Topoisomerases. A conventional DNA relaxation assay was used to investigate the effect of all compounds on human DNA topoisomerases. In these experiments, supercoiled DNA was treated with either topoisomerase I or topoisomerase II in the presence of the test drug at 10 or 50 μM and the DNA relaxation products were then resolved by agarose gel electrophoresis. None of the coumarin derivatives was able to promote DNA cleavage by topoisomerases (data not shown). The amount of nicked (for topoI) or linear (for topoII) DNA species remains very weak in the presence of the arylcoumarin, in contrast to what was observed with the reference drugs camptothecin and etoposide, which produce a high level of single or double strand breaks, respectively. Therefore, the 4-arylcoumarin derivatives cannot be considered as a topoisomerase poisons.

Effects on tubulin polymerization. Figure 1A−C shows the effects of **3**, **8**, and **2** on the turbidimetry time course of microtubule assembly from pure tubulin. A clear inhibition was noted, and the rate of assembly as well as the final amount of microtubules was lower in the presence of **3** and **8** than in the control experiment. Compound **2** had no effect on tubulin polymerization until 26 μM (Figure 1C). In the presence of all three drugs, when the samples were cooled to 10 °C, the polymers depolymerized as well as the control assembled without drugs. The insets of parts A and B of Figure 1 show that the extent of inhibition by **3** and **8**, respectively, increased monotonically with the mole ratio of the total ligand to total tubulin in the solution (*R*). In these figures, 50% inhibition occurred at a mole ratio of 1.45 mol of **3** per mol of tubulin and at a mole ratio of 0.28 mol of **8** per mol of tubulin. A similar experiment performed with combretastatin A-4 showed that a mole ratio of 0.07 mol of combretastatin A-4 per mol of tubulin was necessary to halve the microtubule formation (Figure 1D). Although less potent in tubulin polymerization inhibition, **8** shows, like combretastatin A-4, a substoichiometric mode of inhibition, while **3** is stoichiometric.

Electron microscopy of the polymers remaining with **3** and **8** showed identical normal microtubule structure (data not shown).

The two cytotoxic compounds **3** and **8** inhibit tubulin assembly, whereas the inactive compound **2** shows very little effect in this assay. Interestingly, the most potent compound against tubulin is also, by far, the most potent cytotoxic agent in the series. Although a direct correlation cannot yet be established at this stage, it

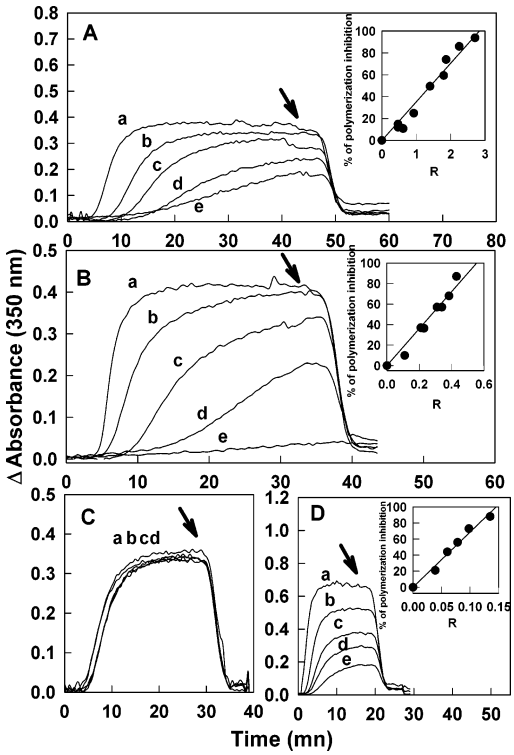

Figure 1. Effect of **3**, **8**, and **2** on the turbidity time course of in vitro microtubule assembly. The reaction was started by warming the solution from 4 to 37 °C. Panel A shows (a) tubulin at 16 μM and (b−e) aliquots of the same solution with 7, 9, 21, and 28 μM of **3**. Panel B shows (a) tubulin at 16 μM and (b−e) aliquots of the same solution with 1.6, 3.2, 4.8, and 6.4 μM of **8**. Panel C shows (a) tubulin at 16 μM and (b−d) aliquots of the same solution with 6.5, 13, 19.5, and 26 μM of **2**. Panel D shows (a) tubulin at 30 μM and (b−e) aliquots of the same solution with 1.2, 1.8, 2.3, 2.9, and 4.0 μM of combretastatin A-4. At the time indicated by the arrow, the samples were cooled to 10 °C. The insets show the percentage of turbidity inhibition as a function of the mole ratio of the total ligand to total tubulin in the solution (R).

seems however plausible that tubulin represents a privileged target for these compounds. Having identified one of the targets, we extended our pharmacology study at the cell level to determine the type of cell death induced by these compounds, principally the two cytotoxic hits **3** and **8**. Different cellular assays were deployed to analyze the effects of the drugs on the cell machinery.

Cell Cycle Effects. Treatment of CEM cells with **3** and **8** for 24 h led to profound changes of the cell cycle profiles, whereas the other compounds had no effect (Figure 2). The flow cytometry analysis of propidium iodide-labeled cells indicates that the two cytotoxic drugs induce a massive accumulation of cells in the G2/M phase. The G2 cell population increases from 23% in the control to 54%, while the G1- and S-phase cell populations gradually decrease from 42% and 33% to 5% and 9%, respectively, in the presence of 1 μM **8**. The G2 block is dose-dependent, as illustrated with **3** in Figure 2b.

In parallel to the G2 block, a characteristic hypodiploid DNA content peak (sub-G1, 32%) can be detected with **3** and **8**. Here again the effect is clearly dose-dependent (Figure 2b). The progressive generation of cells having a hypodiploid DNA content (sub-G1 material) is characteristic of apoptosis and reflects frag-

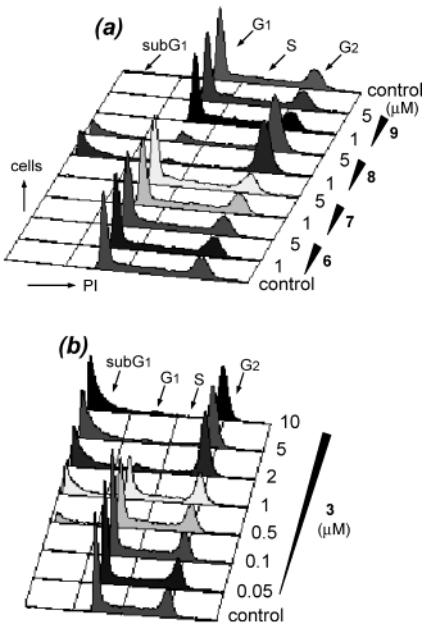

Figure 2. Cell cycle distribution determined by flow cytometry in CEM cells treated for 24 h with (a) 1 or 5 μM compounds **6**−**9** or (b) graded concentration of **3**. Cells were analyzed with the FACScan flow cytometer. Results show a typical experiment which has been repeated three times.

mented DNA. It is not common to see simultaneously the accumulation of cells in the G2- and sub-G1-phases, as these effects are generally sequential.[20] This may reflect an action on two different targets and/or the activation of two independent cell death pathways (as discussed below). Nevertheless, the cell cycle analysis suggests that CEM leukemia cells accomplish apoptosis under treatment with **3** and **8**. Therefore, we went on to examine a variety of apoptotic events using several complementary cytometric and biochemicals methods.

Induction of Apoptosis. (1) Variations of the Mitochondrial Membrane Potential. Mitochondria plays an essential role in the propagation of apoptosis. We used the ampholitic cationic fluorochrome $DiOC_6$ to monitor the changes of the mitochondrial transmembrane potential ($\Delta\Psi_{mt}$) induced by **3** and **8**. CEM cells were treated with graded concentrations of the drugs (50 nM to 10 μM) for 24 h and then analyzed by flow cytometry after $DiOC_6$ labeling. The results are presented in Figure 3.

With both drugs, a population of depolarized cells, characterized by a significant reduction of the cellular uptake of the fluorochrome, appeared gradually as the drug concentration was raised. The decrease of the fluorescence intensity measured with the $DiOC_6$ probe reflects the collapse of $\Delta\Psi_{mt}$, which is a signature for the opening of the mitochondrial megachannels (the so-called permeability transition pores). The effect is reminiscent to that observed with the mitochondrial uncoupling agent CCCP (carbonyl cyanide *p*-chlorophenylhydrazone), a protonophore that abolishes $\Delta\Psi_{mt}$ (Figure 3). The dissipation of $\Delta\Psi_{mt}$ observed with **3** and **8** reflects the opening of the mitochondrial permeability transition pores. This effect, which has been commonly observed with other anticancer drugs irrespective of the cell type, generally defines an early but already irreversible stage of apoptosis.

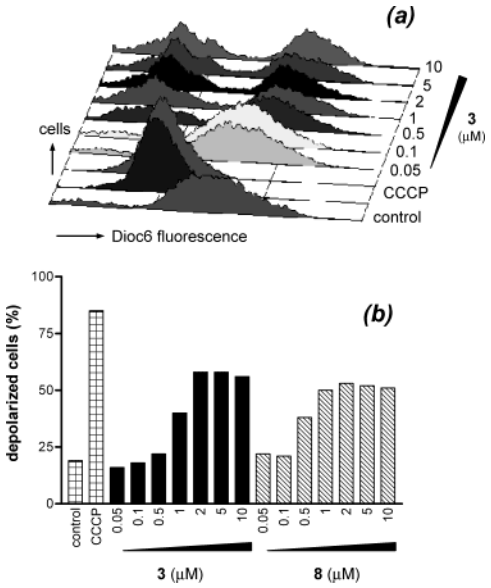

Figure 3. (a) Variations of the mitochondrial membrane potential ($\Delta\psi_{mt}$) measured with the dye $DiOC_6$ (3,3-dihexyloxacarbocyanine iodide**,** 25 nM) in CEM cells treated for 24 h with increasing concentrations of **3**. Parallel experiments were performed with the uncoupling agent CCCP (carbonyl cyanide *p*-chlorophenylhydrazone, 5 and 50 μM for 10 min at 37 °C). (b) The histograms indicate the percentage of depolarized cells measured in the presence of **3** or **8** at the indicated concentration.

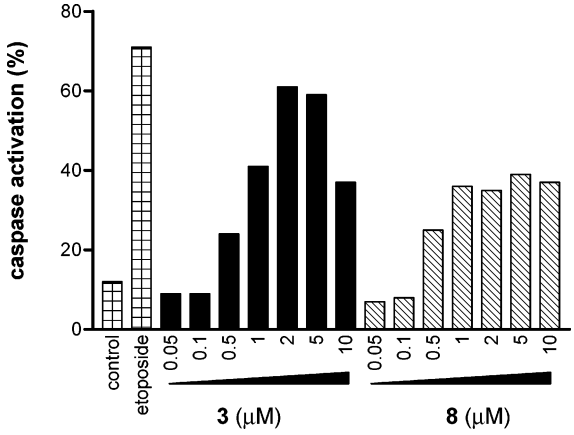

Figure 4. Drug-induced activation of caspase-3 in CEM cells. Cells were exposed to graded concentrations of **3** or **8** (0.05−10 μM) or to etoposide (10 μM) for 24 h prior to the addition of the PhiPhiLux-G_1D_2 probe containing a rhodamine-tagged GDEVDGI peptide motif substrate for caspase-3. Cells were analyzed with the FACScan flow cytometer.

(2) Caspases Activation. Many studies have implicated cysteine proteases (caspases) as key participants in the sequence of events that results in the dismantling of the cell during apoptosis.[21] Therefore, it was interesting to evaluate the effect of **3** and **8** on the activity of caspase-3, one of the major effector caspases. We explored the proteolytic cleavage of the rhodamine-tagged substrate which contains a heptapeptide GDEVDGI recognition sequence for caspase-3 and possibly for other caspases such as caspase-7. As shown in Figure 4, CEM cells treated with **3** showed a massive activation of caspases. The effect is comparable to that of the well-established anticancer proapoptotic drug etoposide. Strong cleavage of the rhodamine-based substrate car-

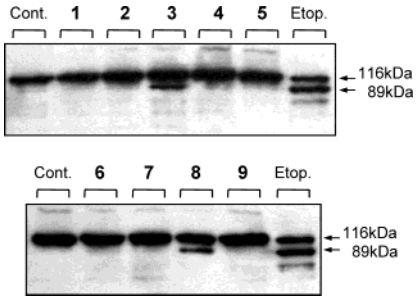

Figure 5. Western blot analysis for the cleavage of PARP. Control lanes (cont) refer to untreated cells. In the other lanes, the cells were treated with the indicated compound at 1 μM for 24 h. In each case, whole cell lysates were subjected to SDS−PAGE followed by blotting with an anti-PARP monoclonal antibody. Etoposide (Etop.) was used at 10 μM. The two arrows point to the full-length PARP (116-kDa band) and the 89-kDa cleavage fragment.

rying the DEVD peptide backbone was also detected with **8** (Figure 4).

Caspase activation was also evidenced by Western blot analysis to monitor the cleavage of poly(ADP-ribose) polymerase (PARP), an enzyme involved in DNA repair that serves as a substrate for caspase-3. As shown in Figure 5, the 116-kDa PARP protein was cleaved into its characteristic 89-kDa fragment upon treatment of the cells with 1 μM **3** and **8** (and with the control drug etoposide) but not with the other compounds. The cleavage of PARP was detected upon treatment of the cells with concentrations of **3** and **8** $\geq$ 0.5 μM (data not shown), i.e. the concentrations for which the hypodiploid peak (sub-G1) starts to appear in the cell cycle experiments. It must be noted, however, that the extent of PARP cleavage always remained limited to about 30−50%, as we could never detect quantitative cleavage of the protein. We are inclined to believe that two cell death mechanisms coexist: one related to apoptosis and the other possibly arising from necrosis. This hypothesis is supported by the following cytometry data.

(3) Loss of Plasma Membrane Asymmetry during Apoptosis. To further characterize the cell death mechanism induced by **3** and **8**, we performed a biparametric cytofluorimetric analysis using propidium iodide and annexin V−FITC, which stain DNA and phosphatidylserine (PS) residues, respectively. Annexin V is a Ca^{2+}-dependent phospholipid binding protein with a high affinity for PS. After the drug treatment, CEM cells were labeled with these two dyes and washed, and the resulting red (PI) and green (FITC) fluorescence was monitored by flow cytometry. As indicated in Figure 6, the percentage of annexin V positive cells slightly increased upon treatment with **3** and **8**. At 2 μM, about 11% of the cells stained positively with annexin V and this cell population, characteristic of an early stage of apoptosis, always remained <17%, even with a higher drug concentration (data not shown). Rapidly, we detected the accumulation of cells doubly stained in green with annexin V and in red by PI, corresponding to late stages of apoptosis and/or dead or necrotic cells. The loss of membrane asymmetry and the ensuing increased accessibility of PS residues to annexin V−FITC is another criteria indicating that the two cytotoxic drugs induce apoptosis, but it is clear from these experiments that compounds **3** and **8** can also cause cell death via a nonapoptotic pathway.

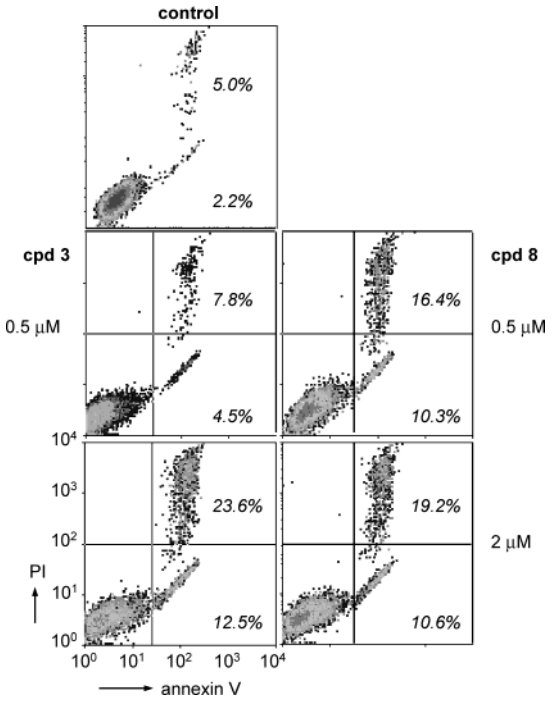

Figure 6. Drug-induced externalization of phosphatidylserine residues. CEM cells were treated with 0.5 or 2 μM **3** or **8** for 24 h and then stained with propidium iodide (PI) and an annexin V−FITC conjugate specifically detecting the exposure of phosphatidylserine (PS) residues at the cell surface. Fluorescence intensities are shown as log scales. In each case, the percentage of annexin-V^+/IP^- cells (lower right square) and annexin-V^+/IP^+ cells (upper right square) is given (±3%). Results show a typical experiment that has been repeated three times.

Altogether, the results give a very consistent picture of the drug mechanism of action. On one hand, there is absolutely no doubt that the newly discovered inhibitors of tubulin assembly **3** and **8** induce apoptosis of the CEM human leukemia cells. The induction of apoptosis is associated with (i) characteristic cell cycle changes (appearance of the sub-G1 population), (ii) loss of the mitochondrial potential membrane ($\Delta\Psi_{mt}$), (iii) activation of caspases-3, and (iv) the loss of membrane asymmetry (annexin V positivity). But in parallel, there is apparently another cell death pathway activated by the two cytotoxic arylcoumarin compounds. This second pathway may explain why **8** is significantly more cytotoxic than **3**, whereas the two compounds perform more or less similarly in terms of drug-induced apoptosis. The high cytotoxic potential of **8** is not directly related to its proapoptotic properties, and another mode of cell killing, as yet undefined, must be implicated.

Conclusion

The two 4-phenylcoumarin derivatives **3** and **8** have been identified as potent cytotoxic agents. The 3′-OH and a 4′-OCH_3 substituents on the 4-phenyl C-ring play an essential role in the cytotoxic action. Compounds **3** and **8** have no effects on human topoisomerases I and II but potently inhibit microtubule assembly. They can therefore be considered as functional analogues of combretastatin A-4, validating thus the design strategy. At the cell level, the two compounds were characterized as proapoptotic agents, but they can also trigger cell death via a nonapoptotic pathway. Compounds **3** and **8**

represent interesting candidates for a preclinical development of novel anticancer agents.

Experimental Section

Chemistry. Melting points were taken on a Büchi capillary apparatus and are uncorrected. NMR spectra were obtained on a Bruker AC 300 spectrometer. Chemical shifts (δ) are reported in ppm for a solution of the compound in $CDCl_3$ with internal reference Me_4Si, and J values are in hertz. Combustion analyses were performed at the Laboratoire de Microanalyse of the Centre National de la Recherche Scientifique, Vernaison, France. Separation by column chromatography was performed using Merck Kieselgel 60 (70−230 mesh). Ether refers to diethyl ether, and petroleum spirit refers to the fraction with distillation range 40−65 °C. All solvents were purified by standard techniques. Arylboronic acids **12**−**15** were prepared by reported procedures involving reaction of the appropriate aryllithium with triisopropylborate.[12,22] 5,7-Dimethoxy-4-trifluoromethylsulfonyloxychromen-2-one **11**,[11] 4-(4′-benzyloxyphenyl)-5,7-dimethoxychromen-2-one **20**,[12] and 4-(4′-benzyloxy-3′-methoxyphenyl)-5,7-dimethoxychromen-2-one **21**[12] were prepared as previously reported.

5,6,7-Trimethoxy-4-trifluoromethylsulfonyloxychromen-2-one 10. Trifluoromethanesulfonic anhydride (3.29 mL, 1.3 equiv) was added dropwise over 10 min to a mixture of the 4-hydroxy-5,6,7-trimethoxycoumarin[13] (3.78 g, 15 mmol) and triethylamine (2.72 mL, 1.3 equiv) in dry dichloromethane (100 mL) at 0 °C. Then the mixture was stirred for 1 h at 0 °C. After dilution with 50% ether−petroleum spirit (200 mL) and filtration through a short pad of silica, the solvent was distilled off under reduced pressure to a small volume (10 mL) and the residue kept at −15 °C overnight. The precipitate was collected and washed with petroleum spirit to afford **10** as fine white needles (5.01 g, 87%): mp 149 °C (EtOH); δ_H 3.88 (3H, s), 3.96 (3H, s), 4.03 (3H, s), 6.14 (1H, s), 6.70 (1H, s); δ_C 56.6 (6-OMe), 61.3, 61.8, 96.3, 102.3, 104.7, 118.6, 139.6, 149.6, 151.5, 157.6, 158.7, 160.1.

4-(3′,4′-Methylenedioxyphenyl)-5,6,7-trimethoxychromen-2-one 5. A mixture of **10** (384 mg, 1 mmol), tetrakis(triphenylphosphine)palladium(0) (25 mg, 2 mol %), lithium chloride (126 mg, 3 equiv), and tributyl-3,4-methylenedioxyphenyltin[15] (452 mg, 1.1 equiv) in dioxane (10 mL) was refluxed overnight. After cooling at room temperature, pyridine (1 mL) was added and the mixture stirred for a further 7 h. The mixture was diluted with ether (50 mL), filtered through a short path of silica, washed with 10% aqueous HCl (3 × 20 mL) and brine (20 mL), and dried over Na_2SO_4. Distillation of the solvent under reduced pressure afforded a white solid which was recrystallized from ethanol to yield **5** as fine white needles (63%): mp 192−193 °C; δ_H 3.37 (3H, s), 3.81 (3H, s), 3.94 (3H, s), 6.03 (2H, s), 6.06 (1H, s), 6.72 (1H, s), 6.81−6.85 (3H, m); δ_C 56.3, 61.1, 61.2, 96.3, 101.3, 107.3, 107.6, 108.5, 114.1, 120.9, 132.7, 139.5, 146.9, 147.6, 151.1, 151.7, 154.9, 156.9, 160.6. Anal. ($C_{19}H_{16}O_7$) C, H.

Coupling of 4-Trifluoromethylsulfonyloxycoumarins with Arylboronic Acids—General Procedure. A mixture of 4-trifluoromethylsulfonyloxycoumarin (1 mmol), tetrakis(triphenylphosphine)palladium(0) (46 mg, 4 mol %), copper(I) iodide (210 mg, 1.1 equiv), sodium carbonate (742 mg, 7 equiv), and arylboronic acid (1.5 equiv) in dry benzene (10 mL) and absolute ethanol (3 mL) was refluxed overnight. Then the reaction mixture was diluted with chloroform (40 mL) and filtered through Celite. The filtrate was washed with a saturated aqueous solution of sodium bicarbonate (3 × 20 mL), and the combined aqueous layers were extracted with chloroform (3 × 20 mL). The organic phases were combined, washed with brine, and dried over Na_2SO_4, and the solvent was distilled under reduced pressure. The residue was crystallized from ether to afford the 4-arylchromen-2-one derivative.

4-(4′-Benzyloxyphenyl)-5,6,7-trimethoxychromen-2-one 16: colorless plates, 69%; mp 130 °C; δ_H 3.27 (3H, s), 3.81 (3H, s), 3.94 (3H, s), 5.13 (2H, s), 6.06 (1H, s), 6.72 (1H, s), 7.01 (2H, d, J 8.7), 7.29 (2H, d, J 8.7), 7.38−7.48 (5H, m); δ_C 56.3, 61.1, 61.2, 70.1, 96.4, 107.4, 114.0, 114.1, 127.6, 128.1, 128.7, 129.0, 131.5, 136.8, 139.6, 151.2, 151.8, 155.2, 156.8, 158.9, 160.8.

4-(4′-Benzyloxy-3′-methoxyphenyl)-5,6,7-trimethoxychromen-2-one 17: fine white needles, 89%; mp 109 °C (MeOH); δ_H 3.27 (3H, s), 3.80 (3H, s), 3.89 (3H, s), 3.94 (3H, s), 5.22 (2H, s), 6.07 (1H, s), 6.72 (1H, s), 6.83 (1H, dd, J 8.3 and 2), 6.88 (1H, d, J 2), 6.92 (1H, d, J 8.3), 7.31−7.48 (5H, m); δ_C 56.1, 56.3, 61.1, 61.3, 71.0, 96.3, 107.3, 111.8, 113.1, 114.0, 119.8, 127.3, 127.9, 128.6, 132.1, 136.9, 139.5, 148.1, 148.7, 151.1, 151.8, 155.1, 156.8, 160.7.

4-(3′-Benzyloxy-4′-methoxyphenyl)-5,6,7-trimethoxychromen-2-one 18: fine light yellow needles, 96%; mp 70 °C (MeOH); δ_H 3.17 (3H, s), 3.78 (3H, s), 3.93 (3H, s), 3.95 (3H, s), 5.17 (2H, s), 6.01 (1H, s), 6.70 (1H, s), 6.90−6.92 (3H, m) and 7.27−7.44 (5H, m); δ_C 56.1, 56.3, 61.1, 61.2, 71.2, 96.4, 107.4, 110.8, 114.1, 114.3, 120.8, 127.4, 128.0, 128.6, 131.5, 137.0, 139.6, 147.1, 149.9, 151.2, 151.8, 155.1, 156.8, 160.8.

4-(4′-Benzyloxy-3′,5′-dimethoxyphenyl)-5,6,7-trimethoxychromen-2-one 19: fine yellow needles, 90%; mp 105 °C; δ_H 3.29 (3H, s), 3.80 (3H, s), 3.83 (6H, s), 3.94 (3H, s), 5.10 (2H, s), 6.10 (1H, s), 6.52 (2H, s), 6.71 (1H, s), 7.27−7.53 (5H, m); δ_C 56.1, 56.2, 61.0, 61.1, 74.9, 96.1, 104.8, 107.2, 113.8, 127.9, 128.1, 128.5, 134.6, 136.4, 137.6, 139.4, 151.0, 151.6, 152.7, 155.2, 156.8, 160.6.

4-(3′-Benzyloxy-4′-methoxyphenyl)-5,7-dimethoxychromen-2-one 22: fine white needles, 96%; mp 184−185 °C (lit.[12] mp 100−102 °C); δ_H 3.33 (3H, s), 3.87 (3H, s), 3.95 (3H, s), 5.13 (2H, s), 5.96 (1H, s,), 6.20 (1H, d, J 2.3), 6.51 (1H, d, J 2.3), 6.84−6.92 (3H, m), 7.32−7.45 (5H, m).

4-(4′-Benzyloxy-3′,5′-dimethoxyphenyl)-5,7-dimethoxychromen-2-one 23: colorless plates, 86%; mp 155 °C; δ_H 3.43 (3H, s), 3.81 (6H, s), 3.87 (3H, s), 5.09 (2H, s), 6.04 (1H, s), 6.23 (1H, d, J 2.3), 6.47 (2H, s), 6.52 (1H, d, J 2.3), 7.30−7.53 (5H, m); δ_C 55.3, 55.7, 56.2, 74.9, 93.6, 95.7, 103.4, 104.7, 112.3, 127.8, 128.1, 128.5, 135.3, 136.4, 137.7, 152.7, 155.4, 157.1, 158.1, 160.7, 163.3.

Removal of the Benzyl Group—General Procedure. A suspension of the substrate (0.5 mmol) in 47% aqueous HBr was stirred at 50 °C for the indicated time. The mixture was then poured into water (50 mL) and extracted with dichloromethane (4 × 20 mL). The organic layers were combined, washed with brine, and dried over Na_2SO_4, and the solvent was distilled off under reduced pressure. The residue was purified by column chromatography (eluant Et_2O) or directly by crystallization from ether to give the corresponding arylcoumarin.

4-(4′-Hydroxyphenyl)-5,6,7 trimethoxychromen-2-one 1: reaction time 12 h; crystallized from ether as light pink plates, 80%; mp 232 °C (AcOEt−Et_2O); δ_H 3.29 (3H, s), 3.81 (3H, s), 3.94 (3H, s), 5.11 (1H, s), 6.06 (1H, s), 6.73 (1H, s), 6.88 (2H, d, J 8.5) and 7.24 (2H, d, J 8.5); δ_C 56.4, 6.13, 96.5, 107.4, 114.1, 114.5, 129.2, 131.3, 139.6, 151.3, 151.8, 155.4, 156.0, 156.9, 161.0. Anal. ($C_{18}H_{16}O_6$) C, H.

4-(4′-Hydroxy-3′-methoxyphenyl)-5,6,7-trimethoxychromen-2-one 2: reaction time 3 h; purified by column chromatography (Et_2O) as fine white needles, 83%; mp 154 °C (from AcOEt−Et_2O); δ_H 3.32 (3H, s), 3.81 (3H, s), 3.90 (3H, s), 3.94 (3H, s), 5.72 (1H, s), 6.08 (1H, s), 6.72 (1H, s), 6.85−6.89 (2H, m), 6.96 (1H, d, J 8.5); δ_C 56.1, 56.3, 61.2, 61.3, 96.4, 107.4, 110.7, 113.6, 114.1, 120.7, 130.9, 139.6, 145.7, 145.9, 151.2, 151.8, 155.3, 156.9, 160.8. Anal. ($C_{19}H_{18}O_7$) C, H.

4-(3′-Hydroxy-4′-methoxyphenyl)-5,6,7-trimethoxychromen-2-one 3: reaction time 3 h; purified by column chromatography (Et_2O) as fine white needles, 79%; mp 157 °C (AcOEt−Et_2O−pentane 1:2:1); δ_H 3.36 (3H, s), 3.80 (3H, s), 3.94 (3H, s), 3.95 (3H, s), 6.06 (1H, s), 6.71 (1H, s), 6.83 (1H, dd, J 8.2 and 2.1), 6.99 (1H, d, J 8.2) and 6.92 (1H, d, J 2.1); δ_C 56.0, 56.3, 61.1, 61.2, 96.3, 107.4, 109.8, 114.1, 114.2, 119.3, 132.3, 139.6, 144.7, 146.7, 151.3, 151.8, 155.2, 156.8, 160.8. Anal. ($C_{19}H_{18}O_7$) C, H.

4-(4′-Hydroxy-3′,5′-dimethoxyphenyl)-5,6,7-trimethoxychromen-2-one 4: reaction time 1 h; crystallized from ether as fine white needles, 88%; mp 205 °C (CH_2Cl_2–Et_2O); δ_H 3.36 (3H, s), 3.81 (3H, s), 3.90 (6H, s), 3.94 (3H, s), 5.62

(1H, s), 6.10 (1H, s), 6.58 (2H, s), 6.72 (1H, s); δ_C 56.2, 56.4, 61.0, 61.2, 96.2, 104.7, 107.2, 113.9, 129.9, 134.8, 139.5, 146.3, 151.0, 151.7, 155.3, 156.8, 160.6. Anal. ($C_{20}H_{20}O_8$) C, H.

4-(4′-Hydroxyphenyl)-5,7-dimethoxychromen-2-one 6. Reaction time 12 h; crystallized from ether as fine white needles, 69%, mp 204 °C (lit.[12] mp 210−213 °C).

4-(4′-Hydroxy-3′-methoxyphenyl)-5,7-dimethoxychromen-2-one 7. Reaction time 3 h; purified by column chromatography (Et_2O) as white needles, 62%, mp 172 °C ($CHCl_3$–Et_2O) (lit.[12] mp 172−173 °C).

4-(3′-Hydroxy-4′-methoxyphenyl)-5,7-dimethoxychromen-2-one 8: reaction time 48 h; purified by column chromatography (Et_2O) as white needles, 74%; mp 152 °C ($CHCl_3$–Et_2O) [lit.[12] mp 153 °C (from EtOH)].

4-(4′-Hydroxy-3′,5′-dimethoxyphenyl)-5,7-dimethoxychromen-2-one 9: reaction time 12 h; crystallized from ether as fine white needles, 96%; mp 215 °C ($CHCl_3$–Et_2O); δ_H 3.51 (3H, s), 3.88 (3H, s), 3.89 (6H, s), 5.62 (1H, s), 6.04 (1H, s), 6.26 (1H, d, *J* 2.5), 6.52 (2H, s), 6.54 (1H, d, *J* 2.5); δ_C 55.5, 55.8, 56.4, 93.6, 95.8, 103.5, 104.5, 112.5, 130.8, 134.8, 146.3, 155.6, 157.2, 158.2, 160.9, 163.3. Anal. ($C_{19}H_{18}O_7$) C, H.

Biology: Topoisomerases Inhibition. The experimental procedure has been previously detailed.[23]

Cell Cultures and Survival Assay. Human CEM leukemia cells were obtained from the American Tissue Culture Collection. Cells were grown at 37 °C in a humidified atmosphere containing 5% CO_2 in RPMI 1640 medium, supplemented with 10% fetal bovine serum, l-glutamine (2 mM), 1.5 g/L sodium bicarbonate, 4.5 g/L glucose, 10 mM HEPES, 1 mM sodium pyruvate, penicillin (100 IU/mL), and streptomycin (100 μg/mL). The cytotoxicity of the test compounds was assessed using a cell proliferation assay developed by Promega (CellTiter 96 AQueous one solution cell proliferation assay). Briefly, 3×10^4 exponentially growing cells were seeded in 96-well microculture plates with various drug concentrations in a volume of 100 μL. After 72 h incubation at 37 °C, 20 μL of the tetrazolium dye was added to each well, and the samples were incubated for a further 2 h at 37 °C. Plates were analyzed on a Labsystems Multiskan MS (type 352) reader at 492 nm.

Preparation of Lamb Brain Tubulin. Tubulin was purified from lamb brain by ammonium sulfate fractionation and ion-exchange chromatography. The protein was stored in liquid nitrogen and prepared as described.[24−26] Protein concentrations were determined spectrophotometrically with a Perkin-Elmer spectrophotometer Lambda 800 and an extinction coefficient at 275 nm of 1.07 L g^{-1} cm^{-1} in 0.5% SDS in neutral aqueous buffer or 1.09 L g^{-1} cm^{-1} in 6 M guanidine hydrochloride.

Tubulin Polymerization. Microtubule assembly was performed in 20 mM sodium phosphate buffer, 1 mM EGTA, 10 mM $MgCl_2$, and 3.4 M glycerol, pH 6.5. The reaction was started by warming the samples at 37 °C in thermostated cuvettes (1 × 0.2 cm), and the mass of polymer formed was monitored by turbidimetry at 350 nm with a Beckman DU7400 spectrophotometer. Samples containing the compound and their controls had less than 2% residual Me_2SO.

Electron Microscopy. Small aliquots of the solution were adsorbed to carbon-coated Formvar films on copper grids, stained for 1 min in 2% uranyl acetate, and observed with a JEOL 1200 electron microscope.

Cell Cycle Analysis. For flow cytometric analysis of DNA content, 10^6 cells in exponential growth were treated with graded concentrations of the test drug for 24 h and then washed with 1 mL of PBS. After centrifugation, the cell pellet was resuspended in 1 mL of cold ethanol for 1 h at 4 °C. The ethanol was removed, the pellet was washed with 1 mL PBS and then incubated for 30 min in a solution of propidium iodide (PI at 50 μg/mL) containing 100 μg/mL RNase. Samples were analyzed on a Becton Dickinson FACScan flow cytometer using the CellQuest software, which was also used to determine the percentage of cells in the different phases of the cell cycle. PI was excited at 488 nm and fluorescence analyzed at 620 nm on channel Fl-2.

Mitochondrial Energization. Mitochondrial energization was determined as the retention of the fluorescent dye $DiOC_6$ (3,3-dihexyloxacarbocyanine iodide, Molecular Probes, Inc.). After the drug treatment, 10^6 cells in 1 mL of complete RPMI 1640 medium were loaded with the probe $DiOC_6$ (usually 25 nM unless otherwise stated) during 30 min at 37 °C prior to the flow cytometric analysis. The same incubation time was applied to the controls and the drug-treated samples. Control experiments were performed by incubating cells with CCCP (carbonyl cyanide *p*-chlorophenylhydrazone) at 5 and 50 μM for 10 min at 37 °C. $DiOC_6$ was excited at 488 nm and fluorescence analyzed at 525 nm (Fl-1) after logarithmic amplification. Forward scattering (FSC) and side scattering (SSC) were analyzed after linear amplification.

Caspase Activation (DEVD cleavage activity). After the drug treatment, the cells were centrifuged, washed with PBS, and resuspended in 50 μL of PhiPhiLux-G_1D_2 substrate (OncoImmunin Inc, MD) for 1 h at 37 °C following the manufacturer's protocol. Cleavage of the peptide linker of PhiPhiLux (sequence DEVD) separates the rhodamine moieties and results in fluorescence detectable by flow cytometry.

PARP Cleavage. Briefly, 7×10^5 exponentially growing CEM cells in complete medium were treated with the test drug at the indicated concentration for 24 h at 37 °C. Cells were pelleted by centrifugation, washed with ice-cold PBS, and resuspended in 100 μL of lysis buffer containing 10 mM Tris pH 7.4, 1 mM sodium vanadate, 1% sodium dodecyl sulfate, 0.1 mM PMSF (added extemporaneously), and the protease inhibitor cocktail ($^1/_{1000}$ dilution, Sigma). Cell lysis was performed for 10 min at 4 °C. The viscosity of the resulting solution was reduced by passage through a 26 gauge needle, prior to measuring the protein content (Bradford method). The protein sample (15 μg), mixed with the loading dye (0.01% bromophenol blue and glycerol), was then boiled to 100 °C for 3 min, prior to electrophoresis on a 7.5% polyacrylamide gel containing 0.1% SDS. Next, for Western blotting, the proteins are transferred onto a Hybond-C nitrocellulose membrane (Amersham) for 90 min at 100 V with a wet transfer system (Biorad). Membranes were blocked with 10% nonfat milk in PBST (0.1% Tween-20, 25 mM phosphate buffer, pH 6.5) for 60 min followed by incubation with anti-PARP polyclonal antibody (Santa Cruz Biotechnology) (dilution 1:1000 in PBST supplemented with 1% nonfat milk) for 60 min. The blots were washed three times (5 min each with PBST) and incubated with a donkey anti-rabbit IgG conjugated to horseradish peroxidase (Santa Cruz Biotechnology, 1:10 000 dilution in PBST containing 1% nonfat milk) for 45 min. After three successive washes with PBST, the Western blot chemiluminescence reagent from NEN (Boston, MA) was used for the detection. Bands were visualized by autoradiography.

Acknowledgment. This work was done under the support of research grants (to C.B.) from the "Ligue Nationale Française Contre le Cancer (Equipe labellisée LA LIGUE)". It was also partially supported by grants from "la Ligue Contre le Cancer" and grants no. 7264 from ARC (to P.B. and V.P.).

References

(1) (a) Jordan, M. A. Mechanism of action of antitumor drugs that interact with microtubules and tubulin. *Curr. Med. Chem.—Anti-Cancer Agents* **2002**, *2*, 1−17. (b) Wood, K. W.; Cornwell, W. D.; Jackson, J. R. Past and future of the mitotic spindle as an oncology target. *Curr. Opin. Pharmacol.* **2001**, *1*, 370−377. (c) Jordan, A.; Hadfield, J. A.; Lawrence, N. J.; McGown, A. T. Tubulin as a target for anticancer drugs: Agents which interact with the mitotic spindle. *Med. Res. Rev.* **1998**, *18*, 259−296. (d) Hamel, E. Antimitotic natural products and their interactions with tubulin. *Med. Res. Rev.* **1996**, *16*, 207−231.

(2) (a) Pettit, G. R.; Cragg, G. M.; Singh, S. B. Antineoplastic agents, 122. Constituents of Combretum caffrum. *J. Nat. Prod.* **1987**, *50*, 386−391. (b) Pettit, G. R.; Singh, S. B.; Boyd, M. R.; Hamel, E.; Pettit, R. K.; Schmidt, J. M.; Hogan, F. Antineoplastic Agents. 291. Isolation and synthesis of combretastatins A-4, A-5, and A-6. *J. Med. Chem.* **1995**, *38*, 1666−1672. (c) Pettit, G. R. Progress in the discovery of biosynthetic anticancer drugs. *J. Nat. Prod.* **1996**, *59*, 812−821.

(3) Gaukroger, K.; Hadfield, J. A.; Hepworth, L. A.; Lawrence, N. J.; McGown, A. T. Novel syntheses of cis and trans isomers of combretastatin A-4. *J. Org. Chem*. **2001**, *66*, 8135−8138 and references therein.
(4) Lin, C. M.; Singh, S. B.; Chu, P. S.; Dempcy, R. O.; Schmidt, J. M.; Pettit, G. R.; Hamel, E. Interactions of tubulin with potent natural and synthetic analogs of the antimitotic agent combretastatin: A structure−activity study. *Mol. Pharmacol.* **1988**, *34*, 200−208.
(5) (a) Cao, S.-G.; Wu, X.-H.; Sim, K.-Y.; Tan, B. H. K.; Vittal, J. J.; Pereira, J. T.; Goh, S.-H. Minor coumarins from Calophyllum teysmannii var. inophylloide and synthesis of cytotoxic calanone derivatives. *Helv. Chim. Acta* **1998**, *81*, 1404−1416. (b) Ito, A.; Chai, H.-B.; Shin, Y. G.; García, R.; Mejía, M.; Gao, Q.; Fairchild, C. R.; Lane, K. E.; Menendez, A. T.; Farnsworth, N. R.; Cordell, G. A.; Pezzuto, J. M.; Kinghorn, A. D. Cytotoxic constituents of the roots of Exostema acuminatum. *Tetrahedron* **2000**, *56*, 6401−6405. (c) Guilet, D.; Seraphin, D.; Rondeau, D.; Richomme, P.; Bruneton, J. Cytotoxic coumarins from Calophyllum dispar. *Phytochemistry* **2001**, *58*, 571−575. (d) Chaturvedula, V. S. P.; Schilling, J. K.; Kingston, D. G. I. New cytotoxic coumarins and prenylated benzophenone derivatives from the bark of Ochrocarpos punctatus from the Madagascar rainforest. *J. Nat. Prod*. **2002**, *65*, 965−972. (e) Jenett-Siems, K.; Kohler, I.; Kraft, C.; Beyer, G.; Melzig, M. F.; Eich, E. Cytotoxic constituents from Exostema mexicanum and Artemisia afra, two traditionally used plant remedies. *Pharmazie* **2002**, *57*, 351−352.
(6) Itoigawa, M.; Ito, C.; Tan, H. T.-W.; Kuchide, M.; Tokuda, H.; Nishino, H.; Furukawa, H. Cancer chemopreventive agents, 4-phenylcoumarins from Calophyllum inophyllum. *Cancer Lett.* **2001**, *169*, 15−19.
(7) Soriano-Garcia, M.; Villena Iribe, R.; Mendoza-Diaz, S.; Del Rayo Camacho, M.; Mata, R. Structure of 4-(3,4-dihydroxyphenyl)-5-(O-*β*-D-galactopyranosyl)-7-methoxycoumarin trihydrate. *Acta Crystallogr.* **1993**, *C49*, 329−330.
(8) Boyle, F. T.; Costello, G. F. Cancer therapy: A move to the molecular level. *Chem. Soc. Rev.* **1998**, *27*, 251−261. Holden, J. A. DNA topoisomerases as anticancer drug targets: From the laboratory to the clinic. *Curr. Med. Chem.—Anti-Cancer Agents* **2001**, *1*, 1−25.
(9) Chang, Y.-C.; Nair, M. G.; Nitiss, J. L. Metabolites of daidzein and genistein and their biological activities. *J. Nat. Prod*. **1995**, *58*, 1901−1902.
(10) Finet, J.-P. Ligand coupling reactions in the synthesis of flavonoids. *Polyphénols Actualités* **2000**, *19*, 18−25.
(11) Boland, G. M.; Donnelly, D. M. X.; Finet, J.-P.; Rea, M. D. Synthesis of neoflavones by Suzuki arylation of 4-substituted coumarins. *J. Chem. Soc., Perkin Trans. 1* **1996**, 2591−2597.
(12) Donnelly, D. M. X.; Finet, J.-P.; Guiry, P. J.; Rea, M. D. Synthesis of *C*-ring hydroxylated neoflavonoids by ligand coupling reactions. *Synth. Commun*. **1999**, *29*, 2719−2730.
(13) Combes, S.; Finet, J.-P.; Siri, D. On the optical activity of the 3-aryl-4-hydroxycoumarin isolated from Millettia Griffoniana: Molecular modelling and total synthesis. *J. Chem. Soc., Perkin Trans. 1* **2002**, 38−44.
(14) Barton, D. H. R.; Donnelly, D. M. X.; Finet, J.-P.; Guiry, P. J. Application of aryllead (IV) derivatives to the preparation of 3-aryl-4-hydroxy-1-benzopyran-2-ones. *J. Chem. Soc., Perkin Trans. 1*, **1992**, 1365−1375.
(15) Barton, D. H. R.; Donnelly, D. M. X.; Finet, J.-P.; Guiry, P. J. A facile synthesis of 3-aryl-4-hydroxycoumarins. *Tetrahedron Lett.* **1989**, *30*, 1539−1542.
(16) Fujimori, A.; Harker, W. G.; Kohlhagen, G.; Hoki, Y.; Pommier, Y. Mutation at the catalytic site of topoisomerase I in CEM/C2, a human leukemia cell line resistant to camptothecin. *Cancer Res*. **1995**, *55*, 1339−1346.
(17) Yamashita, Y.; Kawada, S.; Nakano, H. Induction of mammalian topoisomerase II dependent DNA cleavage by nonintercalative flavonoids, genistein and orobol. *Biochem. Pharmacol*. **1990**, *39*, 737−744.
(18) Lorico, A.; Long, B. H. Biochemical characterization of elsamicin and other coumarin-related antitumor agents as potent inhibitors of human topoisomerase II. *Eur. J. Cancer* **1993**, *29A*, 1985−1991.
(19) (a) Guan, J.; Zhu, X.-K.; Tachibana, Y.; Bastow, K. F.; Brossi, A.; Hamel, E.; Lee, K.-H. Antitumor agents. 185. Synthesis and biological evaluation of tridemethylthiocolchicine analogues as novel topoisomerase II inhibitors. *J. Med. Chem*. **1998**, *41*, 1956−1961. (b) Guan, J.; Zhu, X.-K.; Tachibana, Y.; Bastow, K. F.; Brossi, A.; Hamel, E.; Lee, K.-H. Antitumor agents. Part 186: Synthesis and biological evaluation of demethylcolchiceinamide analogues as cytotoxic DNA topoisomerase II inhibitors. *Bioorg. Med. Chem*. **1998**, *6*, 2127−2131.
(20) Kluza, J.; Lansiaux, A.; Wattez, N.; Mahieu, C.; Osheroff, N.; Bailly, C. Apoptotic response of HL-60 human leukemia cells to the antitumor drug TAS-103. *Cancer Res*. **2000**, *60*, 4077−4084.
(21) Earnshaw, W. C.; Martins, L. M.; Kaufmann, S. H. Mammalian caspases: Structure, activation, substrates, and functions during apoptosis. *Annu. Rev. Biochem*. **1999**, *68*, 383−424.
(22) Ishiurata, H.; Sato, S.; Kabeya, M.; Oda, S.; Suda, M.; Shibasaki, M. PCT Int. Appl. WO 0302537, 2003; *Chem. Abstr*. **2003**, *138*, 89830.
(23) Bailly, C. DNA relaxation and cleavage assays to study topoisomerase I inhibitors. *Methods Enzymol*. **2001**, *340*, 610−623.
(24) Weisenberg, R. C.; Borisy, G. G.; Taylor, E. W. The colchicine-binding protein of mammalian brain and its relation to microtubules. *Biochemistry* **1968**, *7*, 4466−4479.
(25) Lee, J. C.; Frigon, R. P.; Timasheff, S. N. Chemical characterization of calf brain microtubule protein subunits. *J. Biol. Chem*. **1973**, *248*, 7253−7262.
(26) Andreu, J. M.; Gorbunopff, M. J.; Lee, J. C.; Timasheff, S. N. Interaction of tubulin with bifunctional colchicine analogs: An equilibrium study. *Biochemistry* **1984**, *23*, 1742−1752.

JM030903D